Accepted Manuscript

Interaction between natural magnetite sub-micrometric particles and the *Fasciola hepatica* egg: The role of the exposed surface area

Mariana Raineri, Enio Lima, Jr., Marcela Larroza, M. Sergio Moreno, Marcelo Vásquez Mansilla, Juan Sebastián Pappalardo, Roberto D. Zysler

PII: S0014-4894(18)30424-7

DOI: https://doi.org/10.1016/j.exppara.2019.02.006

Reference: YEXPR 7663

To appear in: *Experimental Parasitology*

Received Date: 19 September 2018

Revised Date: 12 February 2019

Accepted Date: 16 February 2019

Please cite this article as: Raineri, M., Lima Jr., , E., Larroza, M., Moreno, M.S., Mansilla, Marcelo.Vá., Pappalardo, Juan.Sebastiá., Zysler, R.D., Interaction between natural magnetite sub-micrometric particles and the *Fasciola hepatica* egg: The role of the exposed surface area, *Experimental Parasitology* (2019), doi: https://doi.org/10.1016/j.exppara.2019.02.006.

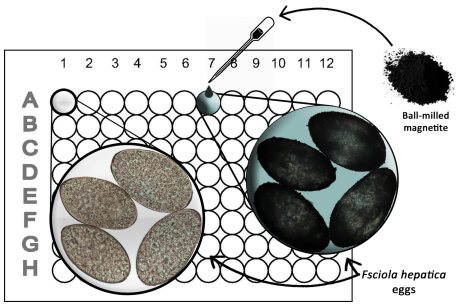

Interaction between natural magnetite sub-micrometric particles and the *Fasciola hepatica* egg: the role of the exposed surface area

Mariana Raineri[1*], Enio Lima Jr[1], Marcela Larroza[2], M. Sergio Moreno[1], Marcelo Vásquez Mansilla[1], Juan Sebastián Pappalardo[2#] & Roberto D. Zysler[1#]

[1]Instituto de Nanociencia y Nanotecnología CNEA-CONICET, Centro Atómico Bariloche, Av. Bustillo 9500, 8400 San Carlos de Bariloche, Argentina

[2]Instituto Nacional de Tecnología Agropecuaria (INTA), Estación Experimental Agropecuaria Bariloche, Grupo de Salud Animal. Bote Modesta Victoria 4450 (8400), S. C. Bariloche, Argentina.

[#], contributed equally as last authors.

[*]Corresponding author:

Dr. Mariana Raineri

E-mail: mariana.raineri@cab.cnea.gov.ar

Phone: 54 294 444 5100

Fax: 54 294 444 5299

Abstract

Fasciolosis is a zoonotic world widely distributed disease caused by the liver fluke *Fasciola hepatica*, which affects animals and occasionally humans. On the other hand, natural iron oxide particles like magnetite are commonly found in soils where they participate in a wide range of environmental processes like organic matter decomposition, the adsorption of ions and molecules, and chemical reactions that involve the participation of soil living microorganisms. Since *Fasciola* eggs become soil components after being released with the infected animal faeces, this study focused on the characterization of the natural interaction between natural sub-micrometric magnetite particles and *F. hepatica* eggs. Our results indicate that particle binding to the *F. hepatica* egg depends on the particle size and it is also related to the exposed surface area since any condition that favors particle agglomeration leads to the reduction of the particle-eggshell binding intensity. Interestingly, this binding was avoided when proteins or phosphate were incorporated to the incubation solution, but not after formaldehyde fixation of eggs. Finally, when eggs were exposed to an external magnet after being incubated with magnetite particles, they were attracted to it without particles being detached, indicating a strong type of bonding between them. Therefore, the results presented here give new insights in order to improve the possibility of harvesting *F. hepatica* eggs by using magnetic materials.

Key words: Magnetite particles, *Fasciola hepatica*, Iron oxides, magnetic particles

1. Introduction

Fasciolosis is a worldwide zoonotic disease caused by the trematode of the genus *Fasciola* (Agarwal & Singh, 1988; Mas-Coma *et al*., 1999, 2005) that infects vertebrate herbivores (e.g., sheep, cattle, goats, horses) that acquire the infection through the ingestion of larval metacercariae encysted on vegetables or suspended in water (Urquhart *et al*., 2001). In humans, infections occur occasionally, but according to the World Health Organization (WHO) they are increasing globally with an estimate of at least 2.4 million infected people in more than 70 countries (WHO, 2007; Cwiklinski *et al*, 2016). *Fasciola hepatica* is highly prevalent in animals destined for human consumption (Mehmood *et al*., 2017) where fasciolosis is considered a disease of highly economic impact because it can cause anemia, weight loss, liver decommission, reduced milk and meat production, poor quality wool, lower fertility rates and deaths to infected animals (Boray, 1969; Dargie, 1987; Hope-Cawdery *et al*, 1977; Morales *et al*., 2000; Moazeni & Ahmadi, 2016; NADIS 2018).

In the life-cycle of *F. hepatica* a final host (animals), an intermediate host (snail of the genus *Lymnaea*) and a carrier (aquatic plants) are involved. The cycle begins when the miracidium penetrates the snail and asexual reproduction occurs forming redia. Redia contains and releases cercariae that exit from the snail and swim up to aquatic or semi-aquatic plants, where they encyst and form infective metacercariae (WHO, 2007). Transmission to other animals and humans occurs when plants are ingested by definitive hosts and metacercariae excyst in the duodenum. Young worms then migrate through the intestinal wall, the peritoneal cavity, and the liver tissue into the biliary ducts, where they develop into adults and start producing immature eggs that are excreted with the faeces (WHO, 2007). *F. hepatica* eggs remain in the soil until a ciliated miracidia develops in approximately 2 to 3 weeks if temperature, humidity and oxygen tension conditions are favorable (WHO, 2007; Moazeni & Ahmadi, 2016).

At the same time, the natural iron-oxides are common soil minerals, since iron is the fourth most abundant element in the earth´s crust (Cornell & Schwertmann, 2003). Iron oxides are originated from magmatic rocks from the earth's surface exposed to aerobic weathering to obtain Fe^{3+} that can be reduced and then reoxidized for precipitation farther away from the original rock or redistributed mechanically by the wind or water and then erosioned in new places (Cornell & Schwertmann, 2003; Colombo *et al*., 2017). Since iron oxides are

thermodynamically stable and possess high energy of crystallization, crystals occur very fast in nature and depending on environmental conditions such as pH, temperature, reduction potential and other factors that alter iron oxides precipitation and dissolution reactions. Therefore, many crystal compositions and even partial replacement of iron for other cations in the structure can be found (Cornell & Schwertmann, 2003).

Natural magnetite is a mix-valence ferromagnetic Fe-oxide with ferrite structure ($Fe^{3+}[Fe^{2+}Fe^{3+}]O_4$) with low solubility but high sorbent capacity for dissolved ions, molecules or gases and high catalytic activity among other characteristics (Cornell & Schwertmann, 2003; He *et al*., 2015). Iron-containing minerals can be used as an environmentally friendly and low-cost catalyst in the remediation of soils and wastewater by accelerating redox reactions for pollutants degradation (Petigara *et al*., 2002; Pereira *et al*., 2012; He *et al*, 2015) and by removing organic contaminants and heavy metals through physical adsorption/desorption processes (Zhang *et al*., 2015). In soils, iron-oxides participate in organic residues decomposition along with soil biota by catalyzing the Fenton reaction (Lyngsie *et al.*, 2018). It is also well known that particle size reduction, or in another words the increase in the surface/volume ratio, leads to an increment in the catalytic capability of magnetite particle, being strongly improved in the submicrometric and in the nanometric size range (Gao *et al*, 2007). The classical Fenton reaction occurs in the presence of reduced iron (Fe^{2+}) and H_2O_2 with the formation of the hydroxyl radical, $^{\bullet}OH$ (Fenton, 1894; Barbusinski, 2009; Lyngsie *et al*., 2018). While the main sources of H_2O_2 are rain waters and soil-living microorganisms (Petigara *et al*., 2002; Lyngsie *et al.*, 2018; Op De Beeck *et al*., 2018), iron reduction in the surface of the oxides are thought to be accomplished by low molecular weight organic compounds with reductive capacity formed during initial soil organic matter decomposition (Lyngsie *et al*., 2018; Op De Beeck *et al*., 2018). In case of ferric iron, another free radical is produced, the hydroperoxyl radical ($^{\bullet}OOH$), in a Fenton-like reaction (Barbusinski, 2009). Free radicals, especially hydroxyl radical, are the main responsible species involved in the degradation process of organic soil material by iron-oxides that are needed for plants and the biomass incorporation of nutrients (Lyngsie *et al.*, 2018; Op De Beeck *et al*., 2018). In this sense, Fenton reactions along with enzymes secreted by soil microbes are essential for soil ecosystem.

Finally, the iron-hydroxide and -oxide surfaces (Fe-OH and Fe-O) can interact with soil components mainly through a complexation reaction at the mineral–water interface with deprotonated groups (e.g. carboxyls and

phenolic hydroxyls) of soil organic compounds (Tombàcz *et al*., 2004; Fink *et al*., 2016; Vindedahl *et al*., 2016). Hence, *F. hepatica* eggs that are present in soils might interact with natural iron-oxides like magnetite particles, and therefore, the main objective of this work was to study the interaction and the variables that influence the binding of submicrometric/nanometric magnetite particles to the egg of *F. hepatica*.

2. Materials and Methods

2.1 Chemicals

Natural magnetite powder was collected from Sierra Grande mining deposits (Río Negro, Argentina) and kindly ball-milled with a high-energy SPEX 8000D mill of the Centro Atómico Bariloche facility during 600 minutes, using a mass ratio between balls and powder of 15:1, and without the addition of solvents or surfactants in the milling procedure. Drugs were purchased either from Anedra (H_2O_2), Biomedicals Inc. ($NaBH_4$); Biopack (Tween-80, Sodium Acetate; Tris base, Sodium Citrate); Cicarelli ($NaHCO_3$; $Na_2B_4O_7.10H_2O$); Fluka (Hydroquinone); Laboratorios Britania S.A. (Hemoglobin); Mallinckrodt Pharmaceuticals Inc. (DMSO, KH_2PO_4, $NaHPO_4$, NaCl and $NaCO_3$); Merck Millipore (Acetic Acid; Citric Acid, Formaldehyde 37%) or Sigma-Aldrich (MES hemi sodium salt, BSA).

2.2 Ball-milled natural magnetite particles: size and morphology

Magnetite samples were conditioned by dispersing 60 µg of particles in 1 ml of dimethyl sulfoxide (DMSO) in a sonicating bath for 1 h. Magnetite particle morphology and size analysis were carried out in a Tecnai F20 G2 transmission electron microscope (TEM) operating at 200 kv coupled with an Energy dispersive X-ray spectroscopy system (EDS), which was used to obtain the elemental composition of the particles. The samples for TEM were prepared by dropping the particle suspension onto carbon-coated copper grids. The Z-average size and the Zeta-potential of natural magnetite at different pH were determined by light scattering in a ZetaSizer 1000 (Malvern Instruments) by adding 4 µl of the magnetite initial dispersion in 1 ml of solution. The electrophoretic mobility data was further processed by the Zetasizer Software 7.11 (Malvern Instruments Ltd.) applying the Smoluchowski equation and the zeta-potential were calculated as an average of three replicates.

118 2.3 Obtention of *F. hepatica* eggs

119 Fecal samples were directly collected from the rectum of a parasitized sheep with *F. hepatica* housed in the
120 INTA-EEA Bariloche facility. Samples obtained on the same day the experiments were performed were
121 subjected to the filtration-sedimentation technique currently used in our laboratory. Briefly, 2-5 g of faeces were
122 homogenized with a mortar and poured through a strainer into a 500 ml conical graduated plastic measuring cups
123 with a narrow bottom in order to concentrate the sediments. Cups were filled by adding tap water and the eggs
124 were allowed to sediment for 10 min. Supernatants were discarded and replaced with fresh water in order to
125 remove fecal debris. Proceeding was repeated three times and then sediments were passed through a sieve of 120
126 μm, rewashed and poured into a Petri dish to be examined with a magnifying glass. *F. hepatica* eggs were
127 carefully removed with a micropipette and placed in distillated water until use.

128 2.4 Preservation of *F. hepatica* eggs

129 After isolation, a total of 100 eggs were fixed overnight at 4 ºC in 4% formaldehyde in 5 mM Acetate Buffer
130 solution (pH 4.0). After fixation, eggs were removed from the fixative solution and placed in a Petri dish
131 containing 10 mM of Phosphate Buffer Saline solution (PBS pH 7.4) for 30 min at 25 ºC. PBS was replaced for
132 water and the formaldehyde-fixed eggs were kept at 4 ºC for a total period of time of 30 days.

133 2.5 Egg binding assay

134 Approximately 10-15 eggs (~10 μl) were placed in a 96 well clear polystyrene microplate (Cat: 655161,
135 Greiner bio-one) containing 180 μl of the solution of interest. Two wells with eggs were needed for each
136 solution since the control (eggs without particles) and the particle-treated group (Eggs + particles) were analyzed
137 at the same time. Eggs were allowed to equilibrate with the solution for 40 min. Then, 10 μl of DMSO was
138 added to the control group and 10 μl of particles (6 mg/ml in DMSO) to the particle-treated group. Incubations
139 were performed under continuous magnetic stirring of the particles at 25 ºC for 15 min. Eggs were separated
140 from the unbound particles with a micropipette, transferred to glass slides and observed by bright field for
141 further image acquisition and quantification of optical density. Eggshell isolation was performed by transferring
142 eggs onto glass slides containing water as a mounting media and applying a slight pressure to the cover slips to
143 open them and force the internal content out. In order to study the particle binding capacity in a protein-

144 containing media we used bovine serum albumin, hemoglobin and a stool from a non-infected sheep solutions
145 containing 0.01% Tween-80 to minimize particle binding to the bottom of the plate. When studying the influence
146 of the pH, solutions were composed of 5mM: Acetic/Acetate solution (Ac, pH 2.5), Citrate Buffer (CB, pH 3.3),
147 MES buffer (pH 6.2), Tris Buffer (TB, pH 7.0), Phosphate Buffer (PB, 7.1 and 8.2); Borate Buffer (BB, 9.0) or
148 Carbonate Buffer (CoB, 10.2) with 0.01% Tween-80. When studying the particle redox potential contribution to
149 the binding process, 10 µl of particles were incubated overnight with 5% of the following solutions in distillated
150 water: $NaBH_4$, Hydroquinone, H_2O_2, NaClO or water itself, washed three times and finally resuspended in 10 µl
151 of DMSO.

152 2.6 Semi-quantification of the bounded number of particles per egg

153 Eggs were observed under light microscopy with a CCD camera for image acquisition with a 40X objective
154 under standard conditions of brightness and magnification. Unequal brightness distribution (shading) was
155 corrected in every image with the a posteriori shading correction plug-in (NIH ImageJ) and optical density was
156 calibrated by using a Kodak No. 3 Calibrated Step Tablet. Then, an automatic optical threshold level was applied
157 to every image in order to delimit the egg area with the wand tool of the software in order to measure the average
158 OD inside the egg. For background correction, an inverse optical threshold was used to measure the average OD
159 of the background area (egg excluded). The final value was obtained by subtracting the background-OD to the
160 egg-OD in every image with the ImageJ software.

161 2.7 Measurement of peroxidase-like activity

162 The peroxidase-like activity of unmilled and ball-milled magnetite particles were determined by degradation
163 of methylene blue dye (Pariona *et al*., 2016). Catalytic oxidation of the dye was evaluated by dispersing 10 mg
164 of particles in 2 ml of 0.01% of methylene blue containing 0.45 M of H_2O_2. In this case the dye was dissolved in
165 5 mM Citrate Buffer (pH 3.3; 0.01% Tween-80) in order to resemble the same conditions of the egg-binding
166 assay of the particles. The catalytic tests were performed in darkness at RT with magnetic stirring of the particles
167 for 30 min. Dye degradation was determined by measuring the absorbance at 665 nm and relating the values of
168 the particle-containing solutions at the end of the experiment (I_t) with the absorbance of the dye solution without
169 particles (I_0) according to the following equation:

Degradation (%) = $(I_t - I_0) / I_0 \times 100$

2.8 Statistical analysis

InfoStat software (Universidad Nacional de Córdoba, Argentina) was used for statistical comparisons. Statistics were performed using non-parametric Wilcoxon-Mann-Whitney or Kruskal-Wallis test. When needed, the software performs the nonparametric multiple comparisons according to Conover (1999). Differences were considered significant if $p<0.05$.

3. Results

3.1 Particle size and morphology

TEM images of the ball-milled particles confirmed a very broad size distribution of non-spherical particles, especially for the larger particles, as it is represented in Figure 1A. A particle-size distribution histogram was created by measuring approximately 50 particles and considering the average length dimension of each particle and after fitting with a Gaussian distribution function, an average particle size (*Mean*) of 186 nm and a standard deviation (*SD*) of 86 nm was obtained (Fig. 1B). TEM images also show particle agglomeration, which is expected as a consequence of the magnetic nature of the particles and the absence of any coating that reduces the interactions among the particles. The chemical composition of the particles was determined by the EDS analysis taking into account at least 5 particles, showing higher proportion of Fe and O atoms and small amounts of Ti and Si. Other elements were occasionally observed in some particles, like Al and Ca, but always in small proportion (data not shown). The presence of other cations in the samples is expected as consequence of the natural origin of the magnetite. However, in small amounts they are not expected to compromise the magnetic properties of the particles or their interaction with the *F. hepatica* eggs.

3.2 Particle-egg interaction determinants

The particle binding capacity to *F. hepatica* eggs in different aqueous conditions are shown in Figure 2. The amount of particles attached to the egg surface was estimated by measuring the optical density of every egg

obtained from a micrograph image analysis. Here, we tested increasing concentrations of NaCl to evaluate if changes in the ionic strength alter the particle-egg interaction (Fig. 2A), a similar analysis was performed for different concentrations of Tween-80 as a model of a non-ionic detergent (Fig. 2B), DMSO as a polar aprotic solvent to help to dissolve polar and non-polar compounds (Fig. 2C) and different solutions containing proteins (Fig. 2D). For the NaCl and the Tween-80 conditions, a marked increase in the optical density in eggs exposed to the particles towards higher concentrations of these additives was observed (Kruskal-Wallis: NaCl: H=95.09, p<0.0001; Tween-80: H=119.08, p<0.0001). For DMSO solutions, no improvement in particle binding was observed at higher concentrations of DMSO, but particle agglomeration seems to happen at above 25% of this compound as it can be observed in the representative images for DMSO in Figure 2C (Kruskal-Wallis: H=41.94, p<0.0001). When DMSO concentrations exceed 50%, *Fasciola* egg integrity was compromised, thus no measurements were carried out at above 50% of DMSO. When egg-particle interaction was evaluated in the presence of protein, a binding decrease was observed except for very low concentrations of BSA (Kruskal-Wallis: H=59.80, p<0.0001).

3.3 Particle agglomeration

In order to analyze the influence of the pH in the interaction between particles and eggs, we evaluated the particle binding capacity to *F. hepatica* eggs when using different solutions of low molarity (5 mM) and different pH (2.5-10.2), as shown in Figure 3A (Kruskal-Wallis: H=206.20, p<0.0001). It can be observed that the particles are capable of binding to the eggs in the whole pH range, excepting for the phosphate-based buffers that exhibits no significant biding activity (p>0.05 vs. Egg control group). Moreover, a significant increment in the binding capability is observed for acidic pH in comparison to the neutral and basic solutions. Hence, in order to determine the role of the electrostatic force attraction and the hydrodynamic size in the egg-particle interaction, DLS measurements of ζ–potential (*Zp*) and *Z*-average size with the respective polydispersity index (*PDI*) were performed at every pH, as given in Figure 3B. It can be observed that the Z-size got smaller as the pH deviated from the neutrality for both acidic and basic conditions and that Z-average sizes were higher than the mean particle-size obtained from the TEM analysis, reflecting the possible formation of agglomerates at near-neutral pH conditions. Similar trends were observed for the PDI with respect to the neutrality. Concerning

220 the particle superficial charge, Zp changed from ~30.4 mV (pH = 3.3) to -14.0 mV (pH = 7) to -37.4 mV (pH =
221 10.2), indicating higher stability at extreme pH values. On the other hand, when observing the mobility of eggs
222 in distilled water through a magnifying glass when an electric field (75 V) was applied, they migrate towards the
223 negative pole, indicating that they are positively charged at neutral pH (data not shown).

224 3.4 Particle redox-state

225 In order to study the influence of the oxidation–reduction of the surface of the particles in the binding to the
226 *F. hepatica* eggs, we pre-incubated ball-milled magnetite particles with different reductive ($NaBH_4$ and
227 Hydroquinone 5%) or oxidant (H_2O_2 and NaClO 5 mM) solutions. As shown in Figure 4, particle binding to
228 eggs is increased for both reduced and oxidized particles, except when using $NaBH_4$ as a reduction agent
229 (Kruskal-Wallis: H=35.62, p<0.0001). This could be due to the fact that evident visible agglomeration of
230 particles was observed after the incubation of particles with this solution and agglomeration seems to decrease
231 the binding capacity. Therefore, this result suggests that changes in surface Fe^{2+}/Fe^{3+} do not to prevent the
232 binding of the particles to the eggs.

233 3.4 Particle size

234 In order to confirm the role of the particle-size in the binding capacity of the particles, the unmilled original
235 natural magnetite and the ball-milled magnetite particles were compared in their binding capacity to eggs (Fig.
236 5). As observed, the ball-milled particles proved to have higher binding activity than the unmilled particles
237 (Wilcoxon-Mann-Whitney, W=28, p=0.0001), reinforcing the latter hypothesis. Also, when Methylene Blue dye
238 degradation was determined, a ~24.8% of reduction in catalytic activity was recorded for the ball-milled
239 magnetite in comparison with a ~5.5% of reduction displayed for the unmilled magnetite confirming the role of
240 the particle exposed area in the interaction with eggs (data not shown).

241 3.5 Eggshell

242 Knowing that the main determinant in the binding interaction for the particle is the exposed surface, an
243 interesting approach would be to recognize the egg component that interacts with the particle. Therefore, we

voided the eggs by applying pressure onto them and then we incubated the eggshells with the particles. As it can be observed in Figure 6, when eggs with particles attached to the surface (Fig. 6A) were cracked (Fig. 6B), the internal content coming from inside the egg was clear of particles, indicating that they do not penetrate to the interior. Moreover, when particles were incubated with cracked and voided eggs (Fig. 6C) they were still able to bind to the surface indicating that the eggshell is the interacting component of the egg with the particles.

3.6 Egg-fixation

Considering that the eggshell is the critical egg component in the egg-particle interaction, we managed to modify the eggshell by fixing them with paraformaldehyde before the incubation step with magnetite particles. As observed in Figure 7, egg fixation did not alter the particle binding but rather maintain it unmodified for at least a month (Kruskal-Wallis: H=60.39, $p<0.0001$).

3.7 Binding strength

Finally, with the porpoise of testing the strength of the binding, after particle adhesion to the egg surface we expose the eggs to a permanent magnet. As it is shown in Figure 8, when an external magnetic field was applied to eggs without particles, they remain in their initial position while eggs with particles bounded to their surfaces were attracted to the magn*et* along with the particles. This finding indicates that particle-egg interaction is strong enough to resist magnetic-induced particle detachment.

4. Discussion

In this work, we showed that ball-milled natural magnetite particles with dimensions of 100-270 nm were able to bind the *F. hepatica* egg surface. Ball-milled magnetite particles have lower structural order and strongly irregular surface in comparison to artificial chemically-produced magnetite nanocrystals (Lima Jr *et al.*, 2010) due to the high-energy milling condition used during particle preparation procedure, which also increases the specific surface area of the particles (Bui *et al.*, 2013). The magnetic nature of the material leads easily to the generation of agglomerates that can reduce their binding capacity to eggs, as it was observed at near-neutral pHs and higher concentrations of DMSO. One possible explanation is that particles might disperse better in NaCl and

Tween-80 aqueous solutions than in DMSO, where particle agglomeration can be observed at the egg surface. On the other hand, particle interaction with eggs was avoided in the case of the protein-containing solutions and in the presence of phosphate ions. In the first case, the decreased interaction could be due to the well know formation of a protein layer (protein corona) on the surface of the iron-oxide particles (Sakulkhu *et al*., 2014), avoiding the direct interaction between the particle and the egg. In the second case, phosphates adsorption at the surfaces of the iron oxides is a well-recognized phenomenon (Nooney, 1996; Choi *et al*., 2016; Fink *et al*., 2016; Zhang *et al*., 2016) that can affect the particle-egg interaction when phosphate buffers are used.

Ball-milled magnetic particles also showed significant binding capacity at neutral and basic pH, although the highest binding capacity was observed in acidic pH. Since higher bindings were found in acidic solutions with positively charged particles and eggs were also positively charged, there must be other factors different from electrostatic attraction that governs the particle-egg interaction, despite some influence of electrostatic attraction could not be ruled out. Even more, in NaCl aqueous solution the particle binding was not masked by the interference of other charged ions but the binding was even more pronounced at higher salinity. On the other hand, higher Zp values were observed in acidic and basic conditions are in agreement with the reduction of the mean particle Z-average size, indicating less degree of agglomeration at non-neutral pH and higher active surface of the particle exposed to interact with the eggs.

Other possibility to be explored is the redox state of the particles. Since ferrite particles and other iron-oxide surfaces are capable to interact with soil organic compounds to participate in Fenton reaction in soil, iron oxides in their ferric state can be reduced by soil microorganisms, as it was described for some brown-root fungi (Lyngsie *et al.*, 2018). Our results indicate that surface oxidation or reduction do not prevent the binding of the particles to the eggs, reinforcing the hypothesis of the exposed surface of the particle as a key-factor that determines the binding activity. Even more, since superficial oxidation is expected to occur during the ball-milling procedure (Lysenko *et al*., 2018), especially when no surfactant, solvent and uncontrolled atmospheric conditions are used, changes in superficial iron state were evaluated through the catalytic peroxidase-like activity of the particles. Because degradation of Methylene Blue dye through Fenton reaction is accelerated when iron is in the Fe^{2+} state (Costa *et al*., 2006), a decrease in the catalytic activity of the milled-particles would indicate

294 particle oxidation during the milling procedure. Since ball-milled magnetite displayed a 24.8% of reduction in
295 catalytic activity and unmilled magnetite only a 5.5%, an increment in superficial Fe^{3+} is not likely to be
296 responsible for the binding improvement of the ball-milled particles and again, the available surface area is still
297 the most likely explanation.

298 Then, we intended to understand the role of *F. hepatica* egg surface in the interaction. *Fasciola* eggshell
299 contain Lysine and arginine (Rzepecki, 1993) so formalin fixing can be achieved in order to modify it. In this
300 case, we did not observe any change in the binding capacity of the particles but rather conservation after egg
301 fixation. On the other hand, *Fasciola* eggshell formation involves tyrosine hydroxylation in proteins of vitelline
302 origin to obtain 3,4-dihydroxyphenylalanine (DOPA) that is further oxidized to quinone in a process known as
303 quinone-tanning or sclerotization process (Rice-Ficht *et al*, 1992; Waite & Rice-Ficht, 1992). Quinones are also
304 likely to interact with iron in nature (Jiang *et al.*, 2015) and they are also candidates for particle binding. In any
305 case, a strong magnetic attraction towards a magnet was observed for eggs with magnetic particles attached to
306 their eggshell, indicating that the particles are strongly attached to the egg surface.

307 So far, results seem to indicate that the exposed surface of the particles and the eggshell are the key elements
308 for the egg-particle interaction. In this sense, some consideration should be done with respect to the chemical
309 interaction between the Fe-oxide and the biological entities in the soil. *F. hepatica* is an hematophagous parasite
310 that lives in the final host from eating hemoglobin to obtain iron (Di Maggio *et al*, 2016) and expresses ferritin in
311 every stage of its life-cycle, especially when the parasite reaches maturity and initiates egg excretion (Cabán-
312 Hernandez *et al*., 2012). Since ferritin expression was demonstrated in soluble egg extracts of *Fasciola* (Moxon
313 *et al*, 2010), one possible explanation that needs to be explored in the future for this interaction to occur could be
314 related to iron obtention for the egg to remain viable in the soil. Nevertheless, the high adsorption capacity of
315 iron-oxides due to their ability to complex deprotonated organic groups cannot be discarded as a non-specific
316 type of interaction (Tombácz *et al*, 2004). Finally, there is one more reflection we would like to make about the
317 fact that some components of the soil biota participates in organic matter decomposition for further nutrient
318 incorporation by intervening in the reduction of iron for Fenton reaction to occur and the production of H_2O_2 as it
319 was mentioned before.

5. Conclusions

Our study provides original results reporting the interaction between natural iron-oxides (like magnetite particles) and the *F. hepatica* eggs and points out the role of the particle active surface as one of the main determinants of the binding. However, given the limited repertoire of research work involving the egg stage of the *F. hepatica* life cycle that occurs in the soil, further investigations must be done in order to explain the exact reason for egg-particle interaction to occur. The results presented here give new insights in order to improve the possibility of harvesting *F. hepatica* eggs by using magnetic materials, as an alternative to the actual sedimentation techniques. In addition, future research is required to understand the interaction between the parasites and the elements present in their natural environment.

Acknowledgements

Dr. Raineri is thankful to CONICET for the postdoctoral fellowship. The authors are indebted to the Argentinean ANPCyT for the financial support through the grant PICT 2015-0883.The authors would like to thank Dr. Fabricio Ruiz from the Department of Materiales Metalicos y Nanoestruturados of the Centro Atómico Bariloche for the ball-milling of the Natural Magnetite; Dr. Carlos Robles and Agustín Martínez from the INTA EEA Bariloche for their expert advice in image acquisition along with Mr. Raúl Cabrera for the technical support. The authors also thank Drs. Gisela Ferraro and Carolina Bagnato (IEDS CONICET) for their collaboration.

References

Agarwal, R.A., Singh, D.K., 1988. Harmful gastropods and their control. Acta Hydrochim. Hydrobiol. 16, 113–138. https://doi.org/10.1002/aheh.19880160202

Barbusinski, K., 2009. Fenton reaction - Controversy concerning the chemistry. Ecol. Chem. Eng. S. 16, 347–358.

342 Boray, J.C., 1969. Experimental fascioliasis in Australia, in: Advances in Parasitology. 7, 95–210.
343 https://doi.org/10.1016/S0065-308X(08)60435-2

344 Bui, T.T., Le, X.Q., To, D.P., Nguyen, V.T., 2013. Investigation of typical properties of nanocrystalline iron
345 powders prepared by ball milling techniques. Adv. Nat. Sci. Nanosci. Nanotechnol. 4, 045003.
346 https://doi.org/10.1088/2043-6262/4/4/045003

347 Cabán-Hernández, K., Gaudier, J.F., Espino, A.M., 2012. Characterization and differential expression of a
348 ferritin protein from *Fasciola hepatica*. Mol. Biochem. Parasitol. 182, 54–61.
349 https://doi.org/10.1016/j.molbiopara.2011.12.005

350 Choi, J., Chung, J., Lee, W., Lim, H.-S., Kim, J.-O., 2016. Recovery of phosphate by magnetic iron oxide
351 particles and iron oxide nanotubes in water. Water, Air, Soil Pollut. 227, 131. https://doi.org/10.1007/s11270-
352 016-2781-7

353 Colombo, C., Iorio, E. di, Liu, Q., Jiang, Z., Barrón, V., 2017. Iron oxide nanoparticles in soils:
354 environmental and agronomic importance. J. Nanosci. Nanotechnol. 17, 4449–4460.
355 https://doi.org/10.1166/jnn.2017.14197

356 Conover, W.J., 1999. Practical nonparametric statistics, 3rd edition. Wiley.

357 Cornell, R., Schwertmann, U., 2003. The iron oxides: structure, properties, reactions, occurrences and uses.
358 2nd ed. Wiley-VCH.

359 Costa, R., Lelis, M., Olivera, L., Fabris, J., Ardisson, J., Rios, R., Silva, C., Lago, R., 2006. Novel active
360 heterogeneous Fenton system based on $Fe_{3-x}M_xO_4$ (Fe, Co, Mn, Ni): The role of M^{2+} species on the reactivity
361 towards H_2O_2 reactions. J. Hazard. Mater. 129, 171–178. https://doi.org/10.1016/j.jhazmat.2005.08.028

362 Cwiklinski, K., O'Neill, S.M., Donnelly, S., Dalton, J.P., 2016. A prospective view of animal and human
363 Fasciolosis. 38, 558–568. Parasite Immunol. https://doi.org/10.1111/pim.12343

364 Dargie, J.D., 1987. The impact on production and mechanisms of pathogenesis of trematode infections in
365 cattle and sheep. Int. J. Parasitol. 17, 453–463. https://doi.org/10.1016/0020-7519(87)90121-4

366 Di Maggio, L., Tirloni, L., Pinto, A.F.M., Diedrich, J.K., Yates, J.R., Benavides, U., Carmona, C., Da Silva
367 Vaz, I., Berasain, P., 2016. Across intra-mammalian stages of the liver fluke *Fasciola hepatica*: A proteomic
368 study. Sci. Rep. 6, 32796. https://doi.org/10.1038/srep32796

369 Fenton, H.J.H., 1894. Oxidation of tartaric acid in presence of iron. J. Chem. Soc. 65, 899–910.
370 https://doi.org/10.1039/ct8946500899

371 Fink, J.R., Inda, A.V., Tiecher, T., Barrón, V., Fink, J.R., Inda, A.V., Tiecher, T., Barrón, V., 2016. Iron
372 oxides and organic matter on soil phosphorus availability. *Ciênc. Agrotec.* 40, 369–379.
373 https://doi.org/10.1590/1413-70542016404023016

374 Gao, L., Zhuang, J., Nie, L., Zhang, J., Zhang, Y., Gu, N., Wang, T., Feng, J., Yang, D., Perrett, S., Yan, X.,
375 2007. Intrinsic peroxidase-like activity of ferromagnetic nanoparticles. Nat. Nanotechnol. 2, 577–583.
376 https://doi.org/10.1038/nnano.2007.260

377 He, H., Zhong, Y., Liang, X., Tan, W., Zhu, J., Wang, C.Y., 2015. Natural magnetite: An efficient catalyst
378 for the degradation of organic contaminant. Sci. Rep. 5, 10139. https://doi.org/10.1038/srep10139

379 Hope-Cawdery M.J, Strickland K.L, C.A. y C.P.J., 1977. Production effects of liver fluke in cattle. The
380 effects of infection on liveweight gain, feed intake and food conversion efficiency in beef cattle. Br. Vet. J. 133,
381 145–159.

382 Jiang, C., Garg, S., Waite, T.D., 2015. Hydroquinone-mediated redox cycling of iron and concomitant
383 oxidation of hydroquinone in oxic waters under acidic conditions: comparison with iron-natural organic matter
384 interactions. Environ. Sci. Technol. 49, 14076–14084. https://doi.org/10.1021/acs.est.5b03189

385 Lima Jr., E., De Biasi, E., Mansilla, M.V., Saleta, M.E., Effenberg, F., Rossi, L.M., Cohen, R., Rechenberg,
386 H.R., Zysler, R.D., 2010. Surface effects in the magnetic properties of crystalline 3 nm ferrite nanoparticles
387 chemically synthesized. J. Appl. Phys. 108, 103919. https://doi.org/10.1063/1.3514585

388 Lyngsie, G., Krumina, L., Tunlid, A., Persson, P., 2018. Generation of hydroxyl radicals from reactions
389 between a dimethoxyhydroquinone and iron oxide nanoparticles. Sci. Rep. 8, 10834.
390 https://doi.org/10.1038/s41598-018-29075-5

391 Lysenko, E.N., Surzhikov, A.P., Nikolaev, E. V., Vlasov, V.A., Zhuravkov, S.P., 2018. The oxidation
392 kinetic study of mechanically milled ultrafine iron powders by thermogravimetric analysis. J. Therm. Anal.
393 Calorim. 134, 307-312. https://doi.org/10.1007/s10973-018-7451-0

394 Mas-Coma, M.S. Esteban, J.G., Bargues, M.D., 1999. Epidemiology of human fascioliasis: A review and
395 proposed new classification. Bull World Health Organ. 77, 340–346.
396 https://doi.org/10.1371/journal.pone.0024567

397 Mas-Coma, S., Bargues, M.D., Valero, M.A., 2005. Fascioliasis and otherplant-borne trematode zoonoses.
398 Int. J. Parasitol. 35, 1255–1278.

399 Mehmood, K., Zhang, H., Sabir, A.J., Abbas, R.Z., Ijaz, M., Durrani, A.Z., Saleem, M.H., Ur Rehman, M.,
400 Iqbal, M.K., Wang, Y., Ahmad, H.I., Abbas, T., Hussain, R., Ghori, M.T., Ali, S., Khan, A.U., Li, J., 2017. A
401 review on epidemiology, global prevalence and economical losses of fasciolosis in ruminants. Microb. Pathog.
402 109, 253-262. https://doi.org/10.1016/j.micpath.2017.06.006

403 Moazeni, M., Ahmadi, A., 2016. Controversial aspects of the life cycle of *Fasciola hepatica*. Exp. Parasitol.
404 169, 81-89. https://doi.org/10.1016/j.exppara.2016.07.010

405 Morales M.A., Luengo J., Vasquez J., 2000. Distribución y tendencia de la fasciolosis en ganado de abasto
406 de Chile. Parasitol. Día. 24, 115–118.

407 Moxon, J. V., Flynn, R.J., Golden, O., Hamilton, J. V., Mulcahy, G., Brophy, P.M., 2010. Immune responses
408 directed at egg proteins during experimental infection with the liver fluke *Fasciola hepatica*. Parasite Immunol.
409 32, 111–124. https://doi.org/10.1111/j.1365-3024.2009.01171.x

410 NADIS, 2018. Liver Fluke Control in Cattle, National Animal Disease Information Service (NADIS). U.K.

411 Nooney, M.G., 1996. A spectroscopic investigation of phosphate adsorption onto iron oxides. J. Vac. Sci.
412 Technol. A Vacuum, Surfaces, Film. 14, 1357. https://doi.org/10.1116/1.579954

413 Op De Beeck, M., Troein, C., Peterson, C., Persson, P., Tunlid, A., 2018. Fenton reaction facilitates organic
414 nitrogen acquisition by an ectomycorrhizal fungus. New Phytol. 218, 335–343.
415 https://doi.org/10.1111/nph.14971

416 Pariona, N., Herrera-Trejo, M., Oliva, J., Martinez, A.I., 2016. Peroxidase-like activity of ferrihydrite and
417 hematite nanoparticles for the degradation of methylene blue. J. Nanomater. 2016, 342780.
418 https://doi.org/10.1155/2016/3427809

419 Pereira, M.C., Oliveira, L.C.A., Murad, E., 2012. Iron oxide catalysts: Fenton and Fenton like reactions – a
420 review. Clay Miner. 47, 285–302. https://doi.org/10.1180/claymin.2012.047.3.01

421 Petigara, B.R., Blough, N. V., Mignerey, A.C., 2002. Mechanisms of hydrogen peroxide decomposition in
422 soils. Environ. Sci. Technol. 36, 639–645. https://doi.org/10.1021/es001726y

423 Rice-Ficht, A.C., Dusek, K.A., John Kochevar, G., Herbert Waite, J., 1992. Eggshell precursor proteins of
424 *Fasciola hepatica*, I. Structure and expression of vitelline protein B. Mol. Biochem. Parasitol. 54, 129–141.
425 https://doi.org/10.1016/0166-6851(92)90106-T

426 Rzepecki, L.M., 1993. Periodicity and sequence degeneration in eggcase precursors (vitelline proteins) from
427 *Fasciola hepatica*. Int. J. Biol. Macromol. 15, 105–108. https://doi.org/10.1016/0141-8130(93)90006-8

428 Sakulkhu, U., Mahmoudi, M., Maurizi, L., Salaklang, J., Hofmann, H., 2014. Protein corona composition of
429 superparamagnetic iron oxide nanoparticles with various physico-chemical properties and coatings. Sci. Rep. 4,
430 5020. https://doi.org/10.1038/srep05020

431 Tombácz, E., Libor, Z., Illés, E., Majzik, A., Klumpp, E., 2004. The role of reactive surface sites and
432 complexation by humic acids in the interaction of clay mineral and iron oxide particles. Org. Geochem. 35, 257–
433 267. https://doi.org/10.1016/j.orggeochem.2003.11.002

Urquhart, G., Armour, J., Duncan, A., Jennings, F., 2001. Parasitología Veterinaria, 2nd ed. Zaragoza, España.

Vindedahl, A.M., Strehlau, J.H., Arnold, W.A., Penn, R.L., 2016. Organic matter and iron oxide nanoparticles: Aggregation, interactions, and reactivity. Environ. Sci. Nano. 3, 494-505 https://doi.org/10.1039/c5en00215j

Waite, J.H., Rice-Ficht, A.C., 1992. Eggshell precursor proteins of *Fasciola hepatica*, II. Microheterogeneity in vitelline protein B. Mol. Biochem. Parasitol. 54, 143–151. https://doi.org/10.1016/0166-6851(92)90107-U

WHO, 2007. Report of the WHO Informal Meeting on use of triclabendazole in fascioliasis control, World Health Organization. Geneva, Switzerland.

Zhang, B., Li, F., Wu, T., Sun, D., Li, Y., 2015. Adsorption of p-nitrophenol from aqueous solutions using nanographite oxide. Colloids Surf. A Physicochem. Eng. Asp. 464, 78–88. https://doi.org/10.1016/j.colsurfa.2014.10.020

Zhang, L., Gao, Y., Xu, Y., Liu, J., 2016. Different performances and mechanisms of phosphate adsorption onto metal oxides and metal hydroxides: A comparative study. J. Chem. Technol. Biotechnol. 91, 1232–1239. https://doi.org/10.1002/jctb.4710

Legends to figures

Fig. 1. Particle characterization. Representative TEM image of the ball-milled natural magnetite showing the morphology of the particles (A) and the corresponding particle-size distribution obtained from the measurement of about 50 particles with the Sturge´s rule. (B). Scale bar 100 nm.

Fig. 2. Characterization of the interaction of particles with eggs under different conditions. Representative images and optical density of *F. hepatica* eggs (n=8-15) incubated with 60 μg of natural magnetic ball-milled particles in DMSO (Egg + P; dark cyan squares) or just DMSO (Egg; black circles) in the following media: NaCl (A), Tween80 (B), DMSO (C) or a protein-containing solution (D). BSA: bovine sera albumin, Hb: hemoglobin. Scale bar 50μm. Statistical significance of Kruskal-Wallis test among different solutions for the Egg+P group are indicated with unshared letters, while differences between Egg+P and the Egg group in the same solution are indicated with # ($p<0.05$). No significant differences were found among different solutions when comparing Egg groups in any condition ($p>0.05$).

Fig. 3. Influence of pH on particle binding capacity and stability. Upper panel (A): Optical density of *F. hepatica* eggs (n=8-15) incubated with 60 μg of natural magnetic ball-milled particles in DMSO (Egg + P; dark cyan squares) or just DMSO (Egg; black circles) in the following pH conditions: Acetic acid (Ac, pH 2.5), Citrate Buffer (CB, pH 3.3), MES Buffer (MES, pH 6.2), Tris Buffer (TB, pH 7.0), Phosphate Buffer (PB, pH 7.1 and 8.2), Borate Buffer (BB, pH 9.0), Carbonate Buffer (CoB, pH 10.2) and distillated water. Statistical significance of Kruskal-Wallis test among different pH conditions for the Egg+P group are indicated with unshared letters while differences between Egg+P and the Egg group at the same pH are indicated with # ($p<0.05$). No significant differences were found among different pH conditions among Egg groups ($p>0.05$). Lower panel (B): ζ-potential (Zp, black squares) and the Z-average size (Cyan bars) with the respective polydispersity index (PDI, fuchsia circles) of the ball-milled particles as function of the pH obtained from DLS measurements.

Fig. 4. The impact of particle oxidation states on egg-particle interaction. Optical density of *F. hepatica* eggs (n=8-15) incubated with 60 μg of magnetite ball-milled particles in distillated water after particle reduction or

474 oxidation. Optical density values are expressed as percent of the control group (particles suspended in DMSO).
475 Statistical significance of Kruskal-Wallis test among different redox conditions are indicated with unshared
476 letters ($p<0.05$).

477 **Fig. 5. Particle-size changes after ball-milling determines the binding to *F. hepatica* eggs.** Optical density of
478 *F. hepatica* eggs (n=8-15) incubated with 60 μg of natural magnetic unmilled or ball-milled particles in Citrate
479 Buffer (5mM, pH 3.3). Statistical significance of Mann-Whitney test (#), $p<0.05$. Scale bar 50μm.

480 **Fig. 6. The interaction of the particles with the eggs depends on the eggshell.** Representative images of intact
481 (A), cracked (B) and empty (C) eggs before (capital letters) and after particle binding (lowercase letter). Scale
482 bar 50μm.

483 **Fig. 7. Binding of particles after formaldehyde-fixation of eggs.** Optical density of formaldehyde-fixed *F.*
484 *hepatica* eggs (n=15) or fresh eggs (Non-fixed) incubated with 60 μg of natural magnetic ball-milled particles in
485 DMSO (Egg + P; dark cyan squares) or just DMSO (Egg; black circles) in distilled water. Statistical significance
486 of Kruskal-Wallis test was found between the Egg + P and the Egg group of the same treatment (#; $p<0.05$). No
487 significant differences were found when comparing different conditions for the Egg and also for the Egg + P
488 group ($p>0.05$).

489 **Fig. 8. Magnetic separation of *F. hepatica* eggs with particles attached to their surface**. A sequence of
490 micrographs of eggs before the exposure to a permanent magnet, a cylindrical magnet of FeNdB with 8000 Oe in
491 the surface (3 cm x 0.3 cm) (A), and after the permanent cylindrical magnet was placed near the Petri dish
492 containing the eggs (B) are shown. Eggs covered with particles are indicated with blue arrows while the eggs
493 without particles are indicated with red arrows in the insets (a, b). Note how eggs without particles remain in the
494 same position while those with particles attached are attracted to the magnet. The lower panel (C-E) shows three
495 images of the eggs covered with particles at the proximity of the magnet from lower (C) to higher magnification
496 (E).

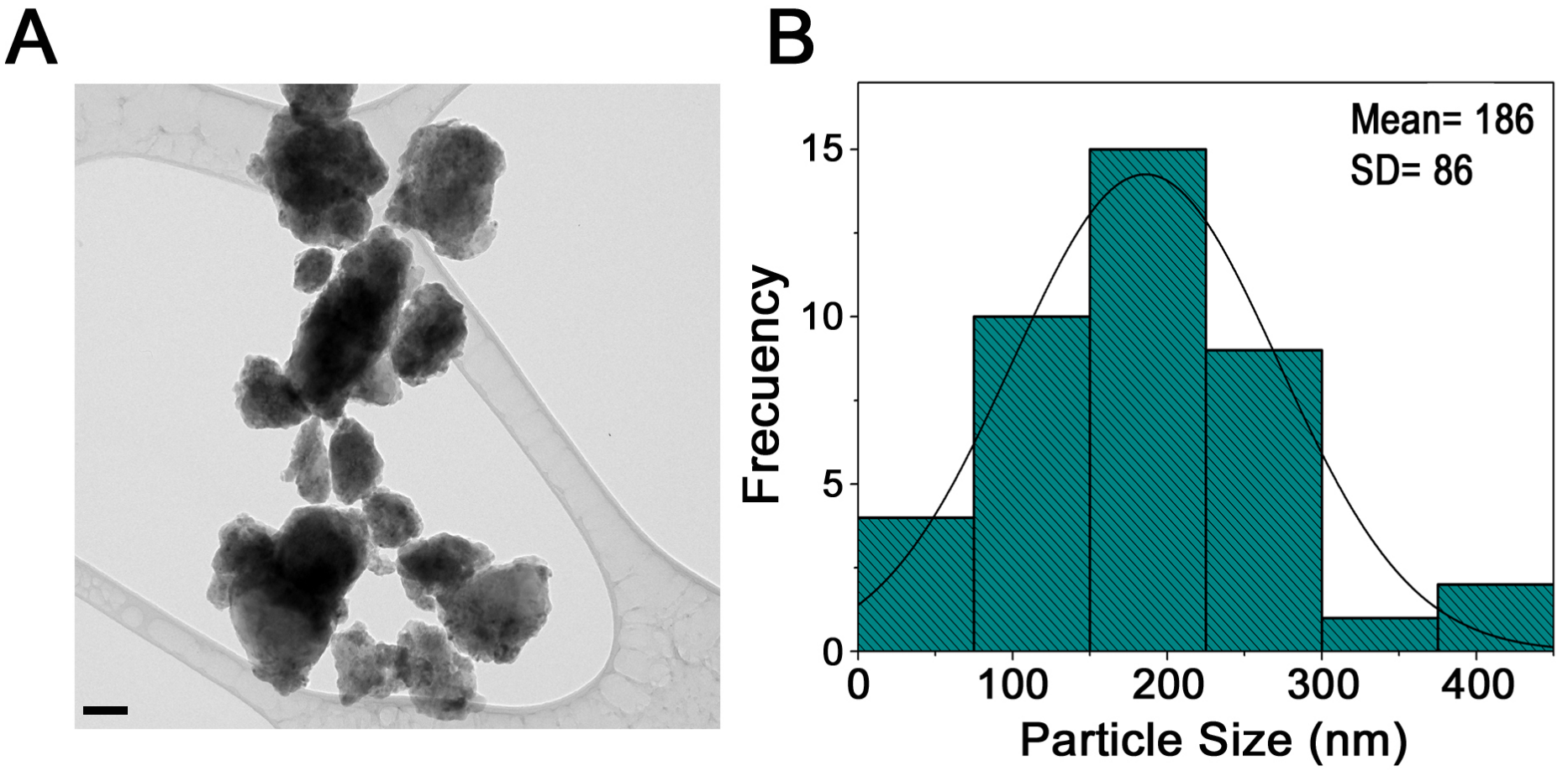
A
B
Mean= 186
SD= 86
Frecuency
Particle Size (nm)
0
5
10
15
0
100
200
300
400

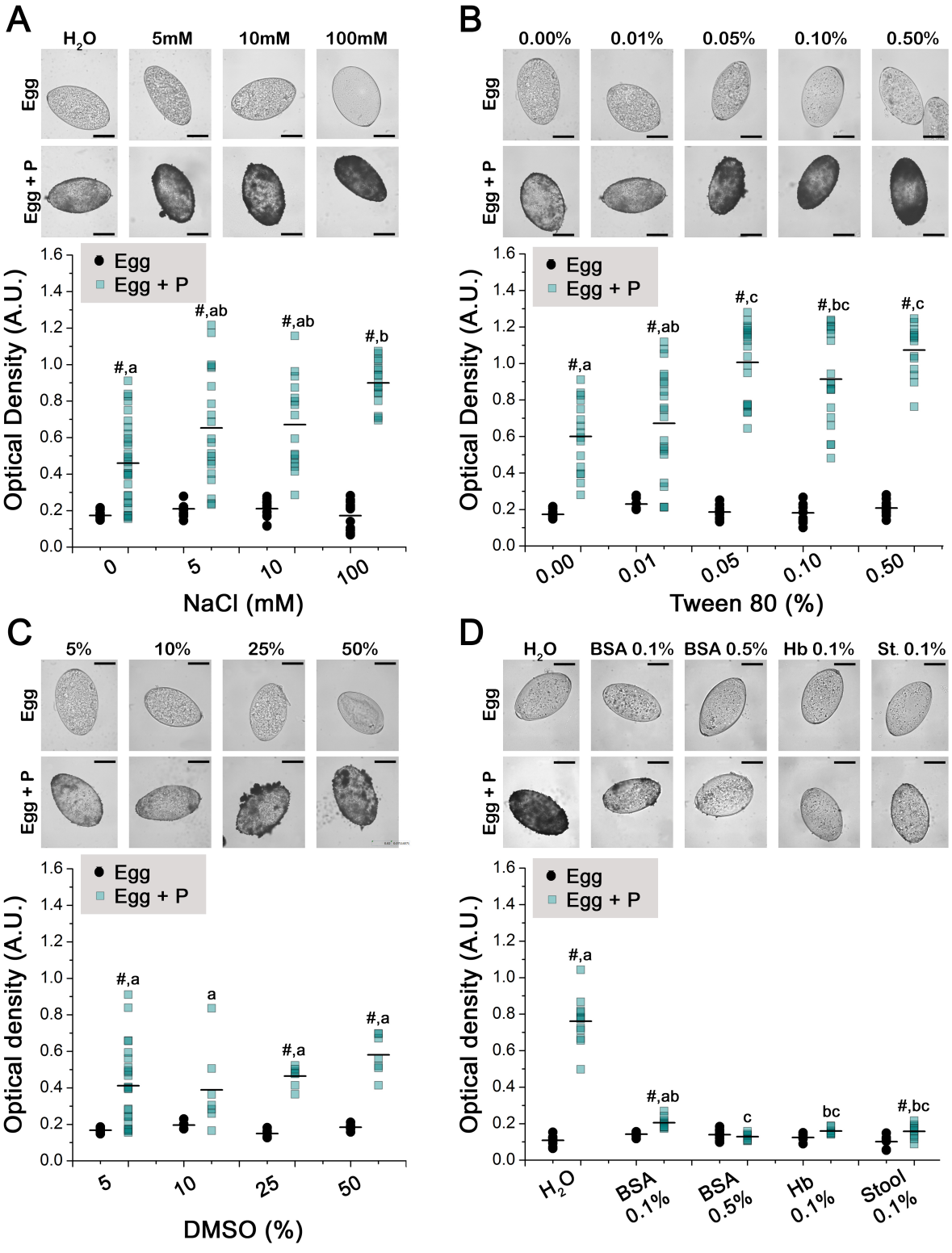
A
H2O
5mM
10mM
100mM
Egg
Egg + P
Optical Density (A.U.)
Egg
Egg + P
#,a
#,ab
#,ab
#,b
0
5
10
100
NaCl (mM)
B
0.00%
0.01%
0.05%
0.10%
0.50%
Egg
Egg + P
Optical Density (A.U.)
Egg
Egg + P
#,a
#,ab
#,c
#,bc
#,c
0.00
0.01
0.05
0.10
0.50
Tween 80 (%)
C
5%
10%
25%
50%
Egg
Egg + P
Optical density (A.U.)
Egg
Egg + P
#,a
a
#,a
#,a
5
10
25
50
DMSO (%)
D
H2O
BSA 0.1%
BSA 0.5%
Hb 0.1%
St. 0.1%
Egg
Egg + P
Optical density (A.U.)
Egg
Egg + P
#,a
#,ab
c
bc
#,bc
H2O
BSA 0.1%
BSA 0.5%
Hb 0.1%
Stool 0.1%

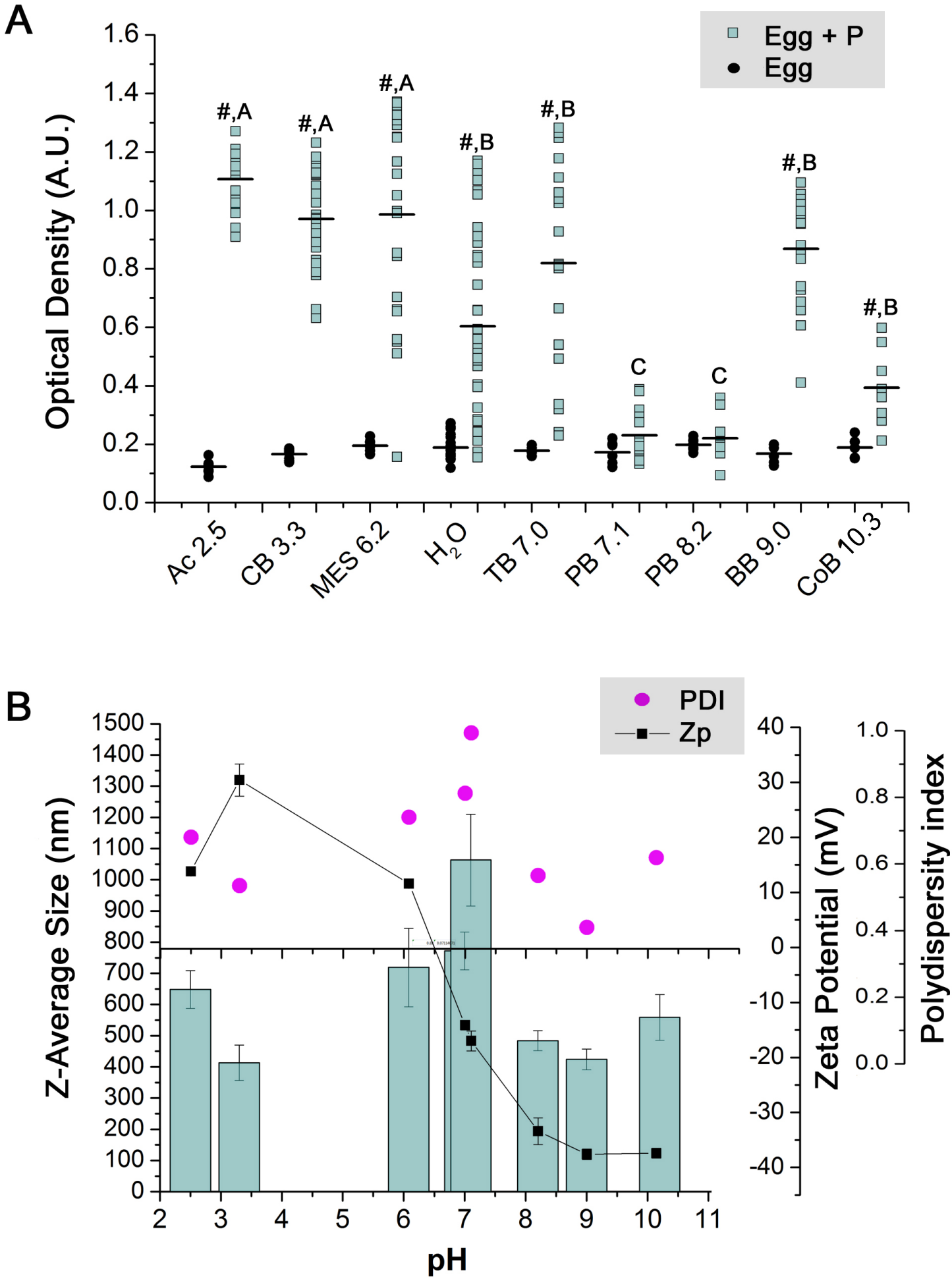
A
Egg + P
Egg
Optical Density (A.U.)
1.6
1.4
1.2
1.0
0.8
0.6
0.4
0.2
0.0
#,A
#,A
#,A
#,B
#,B
C
C
#,B
#,B
Ac 2.5
CB 3.3
MES 6.2
H2O
TB 7.0
PB 7.1
PB 8.2
BB 9.0
CoB 10.3
B
PDI
Zp
Z-Average Size (nm)
1500
1400
1300
1200
1100
1000
900
800
700
600
500
400
300
200
100
0
Zeta Potential (mV)
40
30
20
10
0
-10
-20
-30
-40
Polydispersity index
1.0
0.8
0.6
0.4
0.2
0.0
2
3
4
5
6
7
8
9
10
11
pH

A

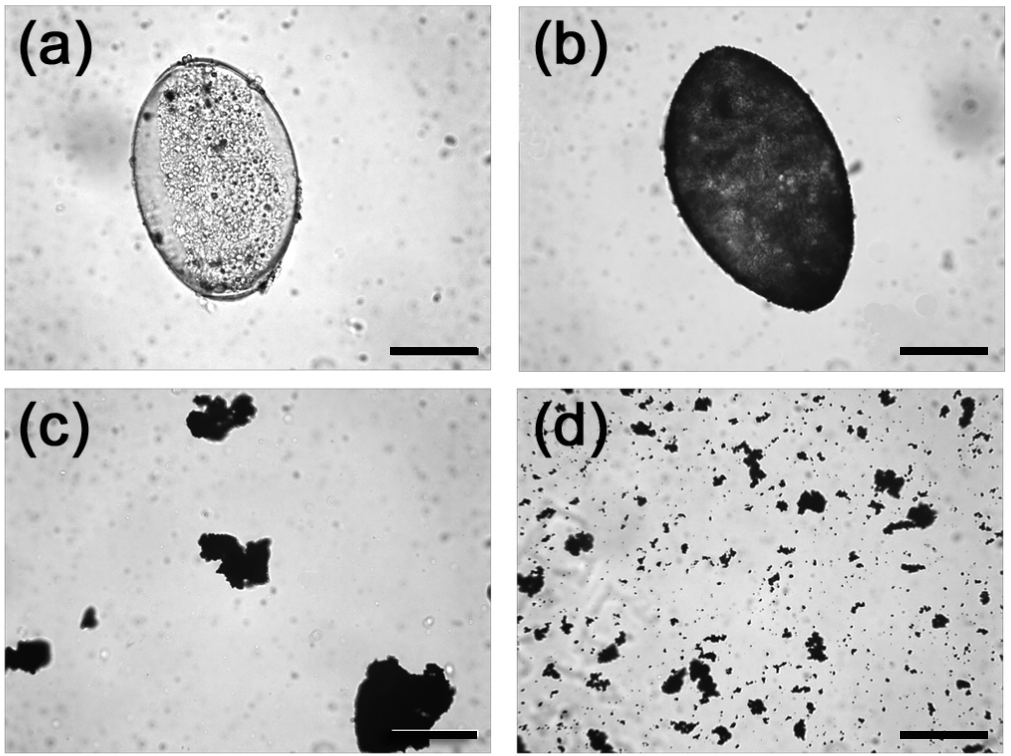
(a)
(b)
(c)
(d)

B

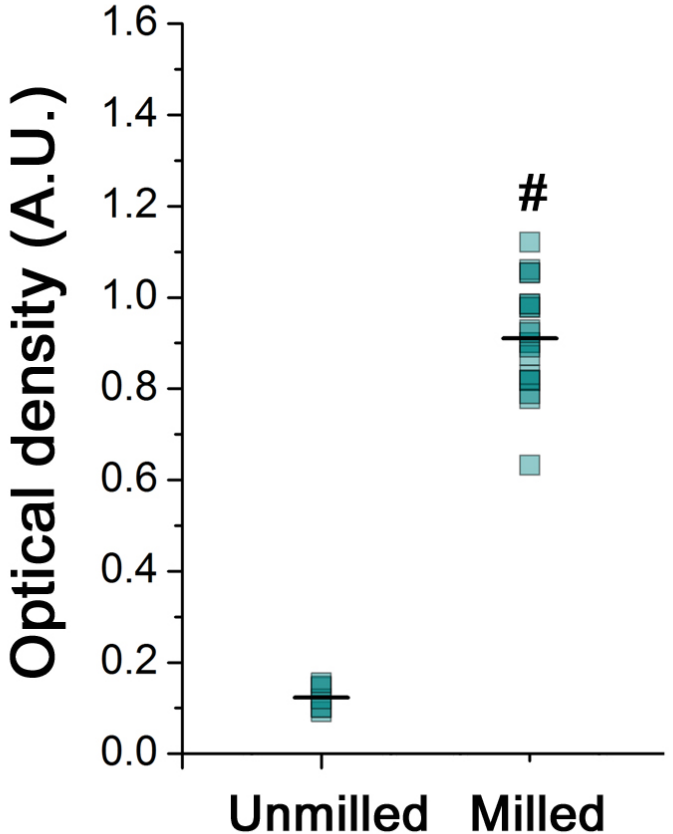
Optical density (A.U.)
1.6
1.4
1.2
1.0
0.8
0.6
0.4
0.2
0.0
#
Unmilled
Milled

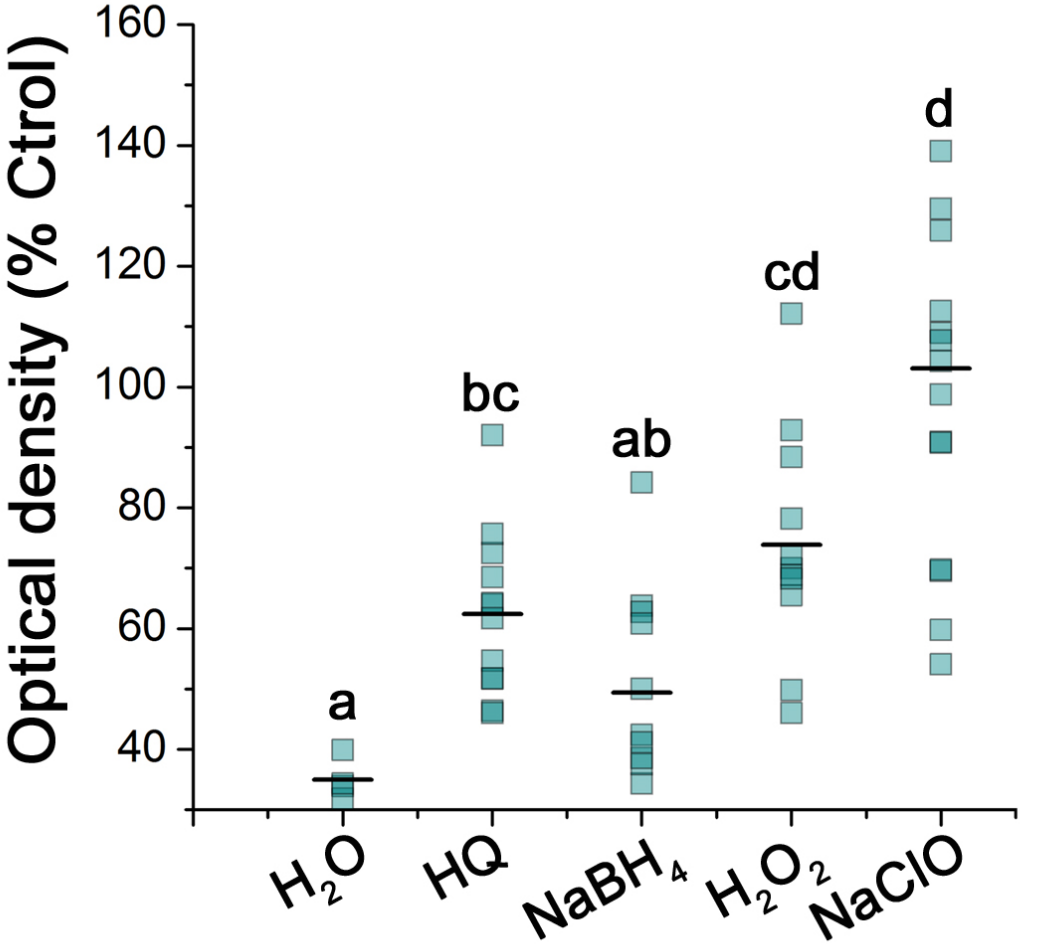
Optical density (% Ctrol)
160
140
120
100
80
60
40
a
bc
ab
cd
d
H2O
HQ
NaBH4
H2O2
NaClO

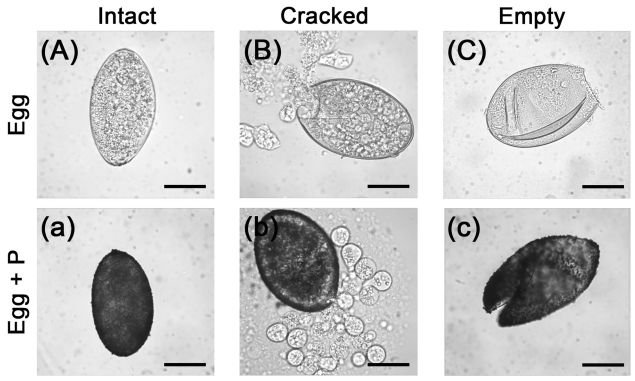

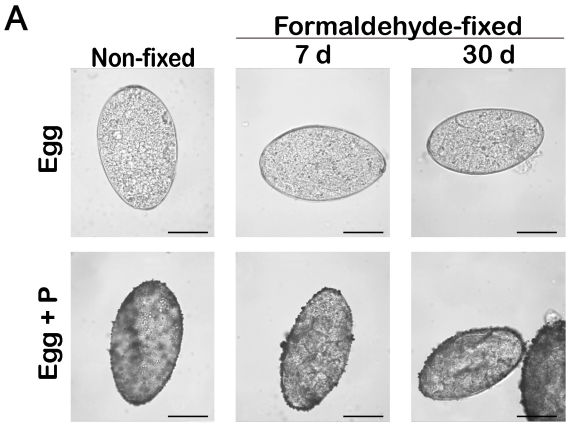

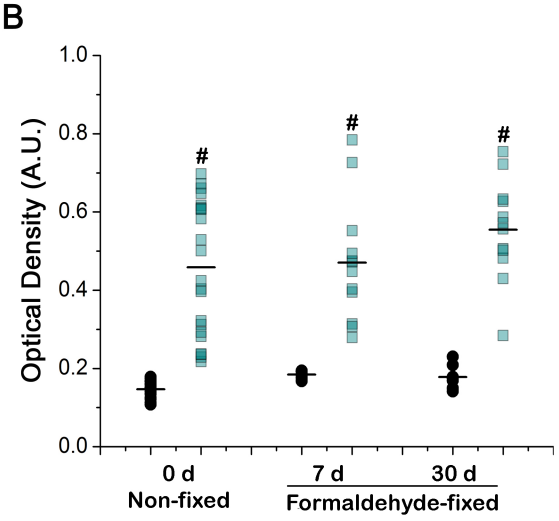

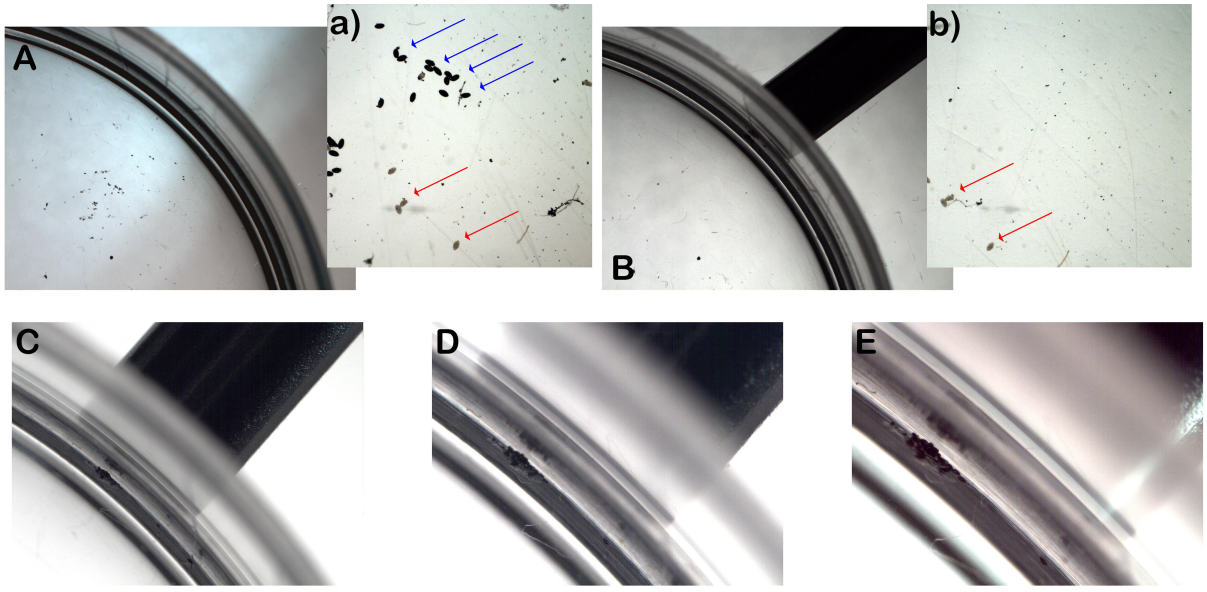

Interaction between natural magnetite sub-micrometric particles and the *Fasciola hepatica* egg: the role of the exposed surface area

- Ball-milled magnetite particles naturally bind to the *Fasciola hepatica* eggshell.
- Particle-egg interaction depends on the particle exposed surface.
- Particle binding to the *Fasciola hepatica* egg surface is not altered when eggs are formaldehyde-fixed but are avoided in the presence of phosphate and proteins.
- Particles are not detached from the egg surface when eggs are exposed to an external magnet.